International Symposium on Nonlinear Theory and its Applications
Xi'an, PRC, October 7–11, 2002

Deterministic stochastic resonance in a noisy environment

Kenichi ARAI, Shin MIZUTANI, and Kazuyuki YOSHIMURA

NTT Communication Science Laboratories, NTT Corporation
2-4, Hikaridai, Seika-cho, Soraku-gun, Kyoto, Japan
Email: ken@cslab.kecl.ntt.co.jp

1. Introduction

There have already been a number of studies on *stochastic resonance* (SR) in a chaotic. One approach employs a chaotic signal as external random excitation instead of noise [1]. Another examines the SR-effects in a chaotic system driven by both noise and a harmonic signal [2]. It has also been reported that, by modulating one of the parameters of a chaotic system, chaotic trajectories hop between two states, e.g., chaotic attractors and periodic orbits [3, 4]. Here, we refer to SR in a deterministic system as *deterministic stochastic resonance* (DSR).

We demonstrated DSR in a modified Rössler oscillator and explained its mechanism [5]. In this paper, we report that DSR can also be observed in a map system as a simple model of a periodically forced chaotic continuous-time oscillator. In addition, we use numerical experiments to show that DSR-like phenomena can be observed in a noisy environment. Then, we discuss the mechanism of noisy DSR.

2. Map system and phase synchronization

As a model for investigating DSR, we study the following two-dimensional mapping [6]

$$x_{n+1} = 1 - a|x_n|, \quad (1)$$

$$\phi_{n+1} = \phi_n + \Omega + \delta x_n + \epsilon \cos(2\pi\phi_n), \quad (2)$$

where $a = 2.0$ and $\delta = 0.1$. Ω and ϵ are both varied. This map is considered to be a simplified model of a periodically forced chaotic oscillator. x_n represents the amplitude of the oscillator and ϕ_n indicates the difference between the oscillator and the periodical force. Ω is interpreted as being the detuning between the period of the autonomous oscillations and the external force. δx_n represents the effect of amplitude fluctuations on the phase rotation and introduces non-uniform phase rotations. ϵ can be regarded as the coupling strength between the oscillator and the force. With a small Ω or a large ϵ, phase locking can be seen in this map, that is, ϕ_n is confined in a chaotic attractor. If we increase Ω or decrease ϵ, ϕ_n can escape from the attractor and ϕ_n grows to infinity with time. This transition from phase entrainment to non-phase entrainment is caused by a crisis [6].

The tent map Eq. (1) has unstable periodic orbits with any length and these orbits can be found analytically. If x_n is exactly on a period-N orbit, the map Eq. (2) is considered to be a simple periodically driven circle map. Classical phase-locking theory (Arnold's tongues) can be applied to the map and then we can obtain the main phase-locked region for each periodic orbit. In the phase-locked region, the trajectories of the phase variable ϕ_n are attracted to a period-N saddle orbit. In addition, there is always a period-N unstable orbit corresponding to each period-N saddle orbit.

Figure 1 shows all the saddle and unstable periodic orbits whose period is less than 12. Circle and cross dots indicate saddle and unstable points, respectively. The left figure shows that the saddle and unstable orbits are completely separated and there is no path connecting the two regions, namely, the phase is locked. As the parameters approach the bifurcation

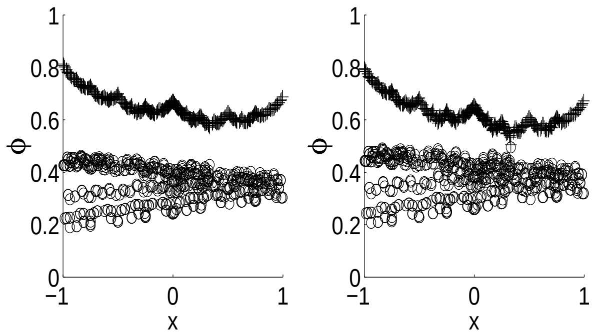

Figure 1: Stable and unstable periodic orbits. $\Omega = \Omega_c + 0.01$ (left), $\Omega = \Omega_c$ (right).

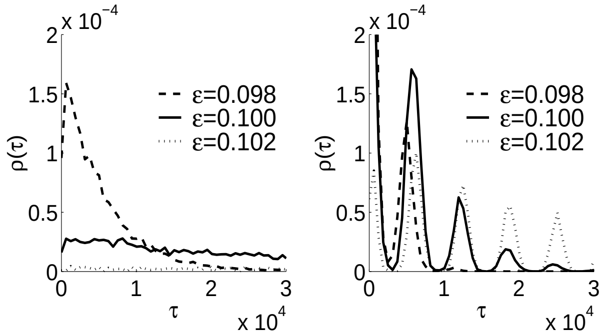

Figure 2: Probability distribution of inter-slip interval with and without signals.

point, the periodic orbits approach each other. At the critical point, the first collision of fixed points occurs, as shown in the right figure. After the parameters exceed the bifurcation value, a path connecting the two regions is formed. This process is the unstable-unstable pair bifurcation, which we also observed in the Rössler attractor. Trajectories can intermittently pass from lower to upper region via the created path. This corresponds to a phase slip in a time-continuous system.

With this map, we can find the exact bifurcation point although we can only find the critical value for the Rössler oscillation experimentally. The two fixed points of the tent map play a crucial role. If the fixed points are phase-locked, all periodic orbits are also phase-locked. Let us focus our attention on the fixed points $x_1^{(1)} = \frac{2}{3}$. The collision occurs at on the line of $\phi = \frac{1}{2}$. Therefore, at the critical point, the parameters have the following relation: $\Omega = \epsilon - \delta x_1^{(1)}$.

3. DSR in a map system

Next, we will see DSR in a map system by adding a harmonic signal: Eq. (2) is modified as,

$$\phi_{n+1} = \phi_n + \Omega + \epsilon \cos(2\pi\phi_n) + \delta x_n + \mu \sin(\omega t), \quad (3)$$

where $\Omega = 0.075$ and $\mu = 0.00375$. Figure 2 shows inter-slip interval distributions. The left figure shows the case when there is no signal. The distributions obey the exponential forms. This indicates that phase slips occur following the Poisson process.

The right figure indicates the distributions with the signal and the distributions have multi-peaks at the integer multiple of the period of the modulation signal. This figure indicates that the phase slips occur in statistical synchronization with the modulation signal: phase slips occur at high probability at a certain phase of the signal.

The system has the DSR effect when the peaks height has one peak as a function of not the external noise intensity but the chaotic fluctuation. We chose ϵ as the parameter controlling chaotic fluctuation. As ϵ increases, phase slips occur more frequently. This is coincident with the fact that slips occur more frequently as the noise intensity increases. Figure 3 shows the difference of the first peaks' heights as a function of ϵ. It can been seen that as ϵ increases

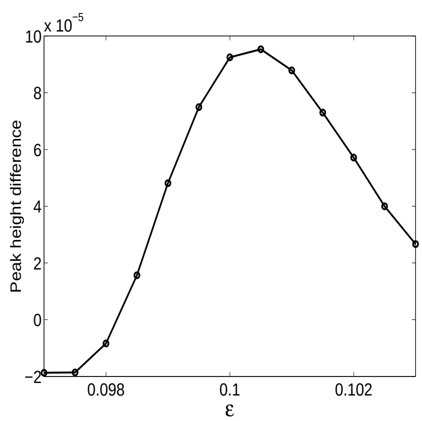

Figure 3: Peak height difference versus ϵ.

the height difference increases until it reaches the maximum point and then it decreases monotonically. There is an optimal ϵ value for the synchronization between phase slips and the modulation signal. This figure verifies the existence of DSR in the map system. Note that the curve in Fig. 3 can be reproduced analytically by the same method as that used for the Rössler oscillator. The map system is a greatly simplified chaotic oscillator but it still has intrinsically the same characteristics in terms of DSR.

4. Noisy deterministic stochastic resonance

It is natural for an input signal to become mixed with noise as it passes through a noisy environment. Thus, we consider that noise, together with the modulation signal, is added to the dynamics of ϕ_n:

$$\begin{aligned}\phi_{n+1} &= \phi_n + \Omega + \epsilon\cos(2\pi\phi_n) + \delta x_n \\ &\quad + \mu\sin(\omega t) + D\xi_n, \end{aligned} \quad (4)$$

where $\Omega = 0.075$, $\mu = 0.0375$ or 0.0, and $\omega = 10^{-3}$. ξ_n is Gaussian white noise: $\langle\xi_m\xi_n\rangle = \delta_{mn}$. As the noise intensity D grows, phase slips occur more frequently. Even if noise is added, the distributions of inter-slip intervals have multi peaks centered at integer multiples of the period of the modulation signals. Figure 4 shows the difference of the first peaks' heights as a function of the parameter ϵ for noise intensity $D = 0.0300$, 0.0375, and 0.0450. Each curve also has a unimodal shape and a maximum point, which indicates that the system can obtain the optimal resonance by the tuning internal fluctuation. This feature is coincident with DSR. As the noise increases, the curve become lower and broader and their peaks move to right. Therefore, as the system receives more noise, it has to move away from the bifurcation point, that is, suppress the chaotic fluctuation to obtain the maximum resonance.

To explain the mechanism of DSR with noise, we have to find the phase slip rate based on mean passage time for each path as a function of the distance between two fixed points and the distance distribution. First, we consider the mean passage time for noise-induced phase slips. Let us focus our attention on the

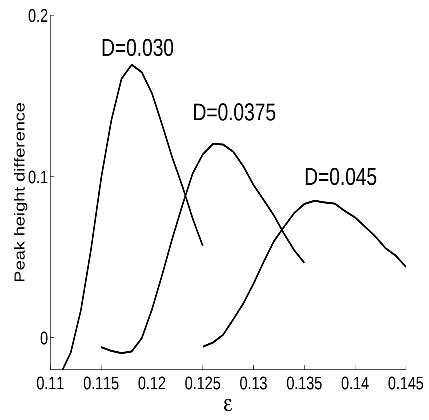

Figure 4: Peak height difference of first peaks versus ϵ for several noise intensities.

motions of ϕ_n with fixed x_n. Since the difference of ϕ_n for one step is sufficiently small, a continuous-time approximation can be applied to Eq. (4) and we have the Langevin process: $\dot{\phi} \sim \Omega' + \epsilon\cos(2\pi\phi) + D\xi(t)$ [7]. We can find the mean passage time $\tau(\phi)$ starting at ϕ by the adjoint Fokker-Plank equation:

$$\{\Omega + \epsilon\cos(2\pi\phi)\}\frac{\partial\tau(\phi)}{\partial\phi} + \frac{1}{2}D^2\frac{\partial^2\tau(\phi)}{\partial\phi^2} = -1. \quad (5)$$

The boundary condition $\tau(1) = 0$ and $\frac{\partial\tau}{\partial\phi}(0) = 0$ indicates that there are absorbing and reflecting walls at $\phi = 1$ and $\phi = 0$, respectively. Equation (5) has the unique solution $\tau(\phi)$ as follows

$$\tau(\phi) = \frac{2}{g^2}\int_\phi^1 dx f(x)\int_0^x \frac{dx'}{f(x')}, \quad (6)$$

where $f(x) = \exp[-2/D^2(\Omega x + \epsilon/2\pi\sin(2\pi x))]$. Provided that starting point ϕ is uniformly distributed from 0 to 1, the mean passage time can be obtained as the average of $\tau(\phi)$ over the whole area

$$\langle\tau\rangle = \int_0^1 \tau(\phi)d\phi. \quad (7)$$

Thus, the mean passage time for crossing two fixed points can be found a function of the parameters ϵ and Ω. We also have to obtain the distribution between pairs consisting of two fixed points. The fixed point distribution, shown in Fig. 1, seems to be fractal and the distribution cannot be obtain analytically.

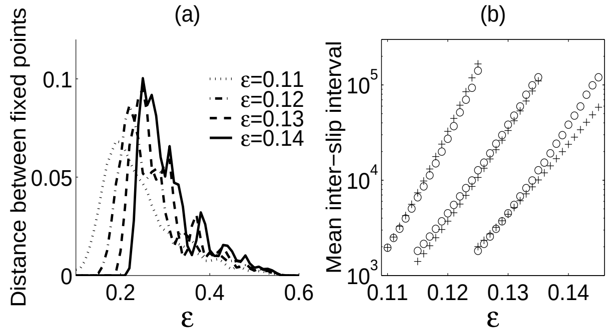

Figure 5: (a) : Distribution of distance of periodic orbits for sevaral ϵ. (b) : Inter-slip interval obtained with Eq. (8) (∘) and numerical simulation (+).

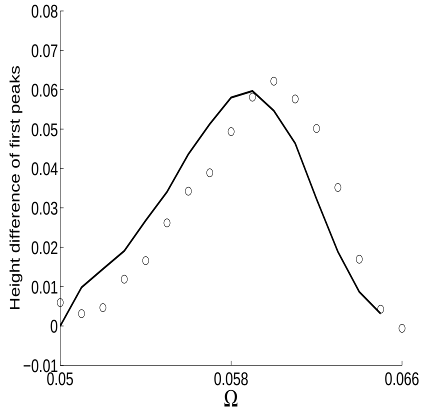

Figure 6: Resonance curve obtained by numerical simulation (∘) and our method (solid line).

Then, the distribution for several values of ϵ was numerically obtained as shown in Fig. 5 (a). If ϵ is greater than the bifurcation point $\epsilon_c = 0.11$, all distances have positive values and phase slips do not occur without noise. As ϵ increases, the distributions move to the right, that is, the distance between fixed points increases.

For given ϵ, Ω, and D values, the mean phase slip rate R of the whole system is found by averaging the passage rates, the inverse of the mean passage time $\langle\tau\rangle$, over all the paths. The distance distribution $P(d)$ is determined by ϵ and Ω and, thus, we have

$$R(\epsilon, \Omega, D) \sim \int \frac{dP(d|\epsilon, \Omega)}{\langle\tau\rangle(\epsilon, \Omega'(d, \epsilon), D)}. \tag{8}$$

In Fig. 5 (b), we compare the mean inter-slip intervals obtained via numerical experiments and Eq. (8) when $\Omega = 0.075$ and $D = 0.030$, 0.0375, and 0.045. The figure shows that there is good agreement between the calculated and experimental results and justifies our approximation of the phase slip rates. Figure 6 shows the resonance curves obtained by the slip rate Eq. (8) and Poisson process approximation, compared with numerical simulation. This also indicates that the curve can be reproduced using the approximate phase slip rate obtained by the mean passage time of noise-induced type-I intermittency and the distance distributions of periodic orbits.

5. Conclusion

We introduced a simple two-dimensional map that shows phase synchronization. DSR is observed in the map, which can be explained by the same mechanism as that of the Rössler oscillator. In addition, the map showed DSR-like phenomena when noise was added to the system. This DSR-like phenomena can be explained by the mean passage rate for noise-induced type-I intermittency and the distance distribution of periodic orbits.

References

[1] E. Ippen, J. Lindner, and W. L. Ditto. *J. Stat. Phys.*, 70:437, 1993.

[2] M. Franaszek and E. Simiu. *Phys. Rev. E*, 54:1298, 1996.

[3] V. S. Anishchenko and M. A. Safanova. *Int. J. Bifurcation and Chaos*, 2:397, 1992.

[4] V. S. Anishchenko, A. B. Neiman, and M. A. Safanova. *J. Stat. Phys.*, 70:183, 1993.

[5] K. Arai, K. Yoshimura, and S. Mizutani. *Phys. Rev. E*, 65:015202, 2002.

[6] A. Pikovsky, G. Osipov, M. Rosenblum, M. Zak, and J. Kurths. *Phys. Rev. Lett.*, 79:47, 1997.

[7] J. E. Hirsch, B. A. Huberman, and D. J. Scalapino. *Phys. Rev. A*, 25:519, 1982.